Engineering Geology 137–138 (2012) 74–84

Contents lists available at SciVerse ScienceDirect

Engineering Geology

journal homepage: www.elsevier.com/locate/enggeo

Digital sieving-Matlab based 3-D image analysis

S. Tafesse [a,*], J.M.R. Fernlund [a], F. Bergholm [b]

[a] Engineering Geology and Geophysics Research Group, Royal Institute of Technology (KTH), Stockholm, Sweden
[b] School of Technology and Health, Royal Institute of Technology (KTH), Stockholm, Sweden

ARTICLE INFO

Article history:
Received 7 July 2010
Received in revised form 29 March 2012
Accepted 1 April 2012
Available online 11 April 2012

Keywords:
Particle form
Particle size
Shape distribution
Image analysis
Digital sieving

ABSTRACT

A new image analysis technique for determining the three-dimensional size and shape distribution of coarse particles has been developed. It entails acquiring a pair of images, one each of the maximum and minimum projected area of the particles. Glow-In-the-Dark beads were used to create luminous background, thus it is named the GID method. In this study the size and shape distribution of four coarse-grained samples, size varies from 2 to 20 cm, have been analyzed. The size distribution of the samples obtained from the GID analysis is comparable to sieve analysis results, and has an extra advantage of being applicable in the field. The algorithm was developed in Matlab; therefore users could make some optimization in the program to meet their own needs as the program code is open source.

1. Introduction

Grain size and shape are the most fundamental properties used to interpret the processes and distance of particle transport in unconsolidated sediments (for example: till, beach and fluvial sediment, and colluvium). It also affects the permeability and angle of friction of the sediment, which are the important factors for determining slope and foundation stability. Particle size and shape analysis is also important to determine the suitability of aggregate materials used in asphalt and concrete construction. The various techniques used to study size and shape distribution of particles can be categorized as indirect (sieving) and direct (manual or image analysis) methods.

Sieving is a simple indirect method that is commonly used in the construction industry to determine the size distribution of granular materials. It does not measure any axial dimension of the particle and the results are highly dependent upon particle shape (Fernlund et al., 2007).

Manual techniques, for example caliper or Danish box methods, are time consuming and prone to operator error. The estimated time required for size measurement using the Danish box is about 20 min for 100 particles (Ibbeken and Denzer, 1998). The number of particles studied using the caliper and Danish-box methods are usually small, roughly 50 to 100 particles are measured per sample. Therefore this method is seldom used to study statistically representative coarse gravel samples; at least 300 particles have to be measured in order to characterize a grain-size distribution of coarse gravel samples (Fripp and Diplas, 1993; Rice and Church, 1996).

The development of a fast and accurate image analysis method for determining the three-dimensional (3-D) size and shape of coarse particles would greatly benefit our ability to interpret the genesis and engineering properties of coarse grained sediments. With the advancement of digital image acquisition techniques and low cost software packages, image analysis methods are developing with great variety. These methods use different instrument setups and various mathematical algorithms to determine the size and shape distribution of particles in a sample. However the existing image analysis methods have limitations in acquiring particle images in the field, and are typically suited to laboratory-based analysis. The size distribution of the sample determined from some of the existing image analysis methods is not easily comparable with sieve analysis results. This paper has three main objectives: (1) to describe a new digital-sieving procedure, the GID method which is suitable for acquiring particles image in the field, (2) to assess its performance, especially by comparing GID grain size information to the results with mechanical sieving and (3) to discuss the subsequent advantages of the GID method over the existing image analysis methods.

2. Background

The grain size and shape distribution in unconsolidated sediments varies dramatically, depending upon provenance, mineral composition, mode of transport and deposition of the constituent particles. Although the concept of size and shape of a particle is not easy to describe in simplified terms, there are several definitions based on the different methods of measurement.

The size of a spherical object can be unambiguously quantified by its diameter, and likewise regularly shaped objects such as cubes and

* Corresponding author. Tel.: +46 8 790 6807; fax: +46 8 790 7045.
E-mail addresses: tafesse@kth.se (S. Tafesse), joanne@kth.se (J.M.R. Fernlund), fredrik.bergholm@sth.kth.se (F. Bergholm).

0013-7952/$ – see front matter © 2012 Elsevier B.V. All rights reserved.
doi:10.1016/j.enggeo.2012.04.001

dodecahedra can be described with one dimension. If the particles in unconsolidated sediment were all regular in shape, no difficulties would arise in determining their size (Pettijohn, 1984). However particles in sediments are irregular and non-spherical in shape.

2.1. Particle size

The size of a particle is often represented with the three axes (length, width and thickness); but these axes are defined and measured in various ways. Numerous notations have been used to describe the three axes of the particles; the most used representations are: a, b and c (Zingg, 1935; Krumbein and Pettijohn, 1938), and L, I and S (Sneed and Folk, 1958).

There are several methods that have been used to define the complex concept of size for irregular particles (Wadell, 1935; Zingg, 1935; Krumbein, 1941; Folk, 1966; Allen, 1968; Pettijohn, 1984; Ibbeken and Denzer, 1998). Some researchers define the length as the maximum caliper dimension (a-axis), and then measured the width (b-axis) and thickness (c-axis) as orthogonal dimensions to the a-axis. Therefore both b and c-axes of the particle are linked to the position of the maximum dimension; if the a-axis is determined then the c-axis is the smallest of the two perpendicular intercepts of the particle that is located in the direction perpendicular to the maximum dimension. In geology it is common that the length and width is defined as the dimensions of the sides of the smallest circumscribed box around the particles largest projected area and the thickness as the longest measure perpendicular to the rectangle (Griffith, 1967). In this case the longest axis is not the longest three-dimensional (3-D) sizes. This measurement is quite subjective; because it is difficult to determine both the largest projected area and the smallest circumscribing rectangle.

There are several ways to measure the axes of the particles. In general, two main methods are used today: size based on the axial dimensions of particles, and sieve size.

2.1.1. Size with manual measurements

The manual measurement techniques were developed where each particle is evaluated and measured by hand, such as using Danish-box or caliper. These methods are quite subjective. One reason is that it is difficult to determine what to measure; to determine the smallest rectangle or the longest 3-D length. With computers it is now possible to determine the size and shape of particles using modern image analysis methods.

2.1.2. Image analysis size

Particle dimensions can be measured objectively through image analysis methods, which comprises acquiring images of the particles and the analysis is done using some software that quantifies the "parameters" defined by the software. However, some sources of error may arise from the image acquisition setup and definition of parameters used in the algorithm.

Several image analysis methods consist of mechanical setups; most of which have little control on which aspects of the particles are imaged. The orientation of the particle in the image may not allow measurement of the major aces (longest, intermediate and shortest axes) but instead only apparent axial dimensions. Moreover, imaging rock samples which often consist of both light and dark color particles is challenging; as it is not easy to use a uniform background and thus produce images of sufficient quality. Often preprocessing is necessary which can introduce another source of error.

In different image analysis methods the predefined parameters and algorithms used to compute particle size can vary quite extensively. Thus, results vary between different methods (Wang and Fernlund, 1994). Some of the numerous, techniques used to quantify the axes of the particle are: the length of the sides of the smallest bounding box around the particle image, the diameter of a best fit ellipse around the particle, or the Feret diameter.

Image analysis methods have many advantages over the manual measurements. The measurement are objective, can be done faster and all the particles are measured (Lindqvist and Åkesson, 2001; Hayakawaa and Oguchib, 2005). However one needs to keep in mind that there is a margin of error in the results (Lindström, 2010).

2.2. Sieve size

Sieve size of a particle is related to the size of the square aperture which allows the particle to pass. It is measured based on the mass of all the particles retained on a sieve compared to the total mass of the sample. It is not a good size descriptor as it does not measure the axial dimension of a particle (Fernlund et al., 2007). Furthermore the results are dependent upon the particle shape; for elongated and flat particles a sieve analysis will not yield a reliable measure (Allen, 1968; Pettijohn, 1984; Syvitski, 1991; Fernlund, 1998; Fernlund et al., 2007). Beside the particle shape, sieve analysis results are dependent on many factors, such as the number of sieves used, the initial sample size placed in the stacked sieves, and the duration and method of shaking.

2.3. Shape of particle

The aspects of particle shape are defined in different ways (Zingg, 1935; Krumbein and Pettijohn, 1938; Sneed and Folk, 1958; Griffith, 1967; Gordon et al., 1992; Bunte and Abt, 2001; Drik, 2008). The shape of both natural and crushed aggregate materials is not uniform; it has quite complex morphologies. Although the nomenclature used in this field is not commonly agreed upon; shape can be described in terms of three main descriptors (Evans and Benn, 2004): form, roundness and surface texture (Figure 1a).

Form is commonly referred to as shape without regard to roundness and surface texture. It reflects the gross morphology of the particle (Gomez et al., 1988; Evans and Benn, 2004) (Figure 1a). It depends on the relative dimensions of the three axes, and can be expressed by various relationships of the axial ratios of a particle. According to the axial ratios, the particles can be classified into different classes. The terminology varies, for example: 'flat', 'spherical', 'flat and columnar' and 'columnar' (Zingg, 1935), renamed by Krumbein and Pettijohn (1938) as 'disk shaped', 'spherical', 'bladed' and 'rod-like' (Krumbein and Pettijohn, 1938; Krumbein, 1941). Brewer (1964) also made further modifications and renamed the classes 'oblate', 'equant', 'bladed' and 'prolate'. This is refined again by Bunte and Abt (2001):

- An equant shaped particle has almost identical a, b, and c axes.
- A bladed like particle is thin and long, the two axial ratios c/b and b/a are small,
- An elongated particles are long, which has a small b/a ratios but large c/b ratios.

Particle form is often plotted on the Zingg or Sneed and Folk diagram (Figure 1b and c) (Zingg, 1935; Sneed and Folk, 1958).

Roundness is a large scale smoothness which describes how well the edges of a particle are curved to a rounded shape (Figure 1a). It is a more difficult parameter to quantify than the particle form. Wadell (1932) developed a complicated procedure to quantify roundness (P) as the average of the radii (r) that can be fitted into all corners (curvatures) divided by the radius of the largest inscribed circle (R) (Figure 1d).

$$P = (\sum r_n)/(n \cdot R). \quad (1)$$

Numerous researchers have proposed image analysis methods to measure roundness (angularity) of a particle (Blum, 1967; Kwan et al., 1999; Masad et al., 2000; Rao and Tutumluer, 2000; Masad et al., 2001; Rao et al., 2002; Wang et al., 2005; Al-Rousan et al., 2007; Masad et al., 2007). However most of them do not provide acceptable accuracy (Tafesse et al., submitted for publication). Therefore the majority of

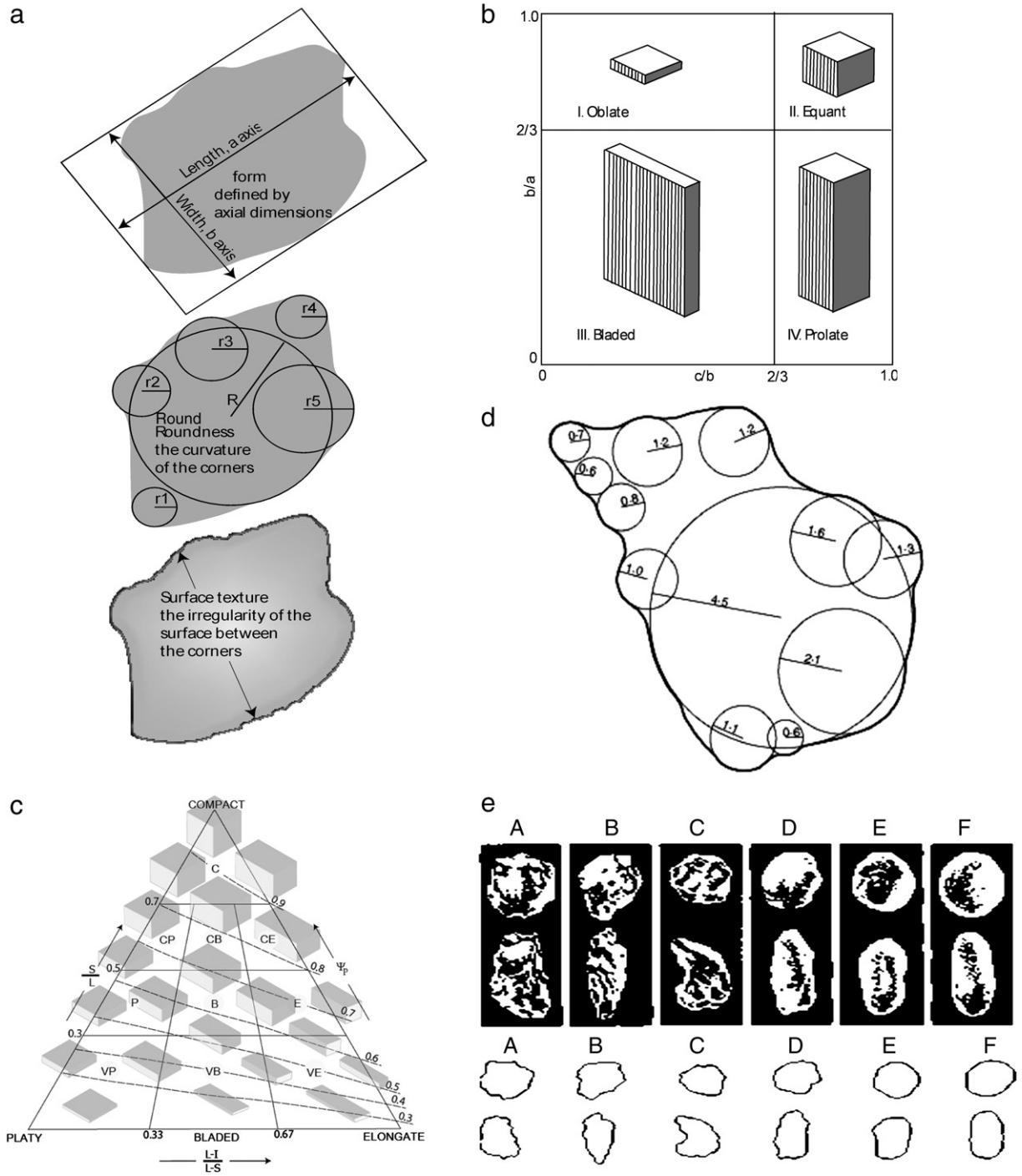

Fig. 1. Different ways of representing morphological features.a. Three morphological descriptors of particle shape,b. Form classification bi-variant diagram, modified after Zingg (1935): a = length, b = breadth and c = thickness,c. Sneed and Folk (1958) form classification triangular diagram: L = length, I = intermediate axis (breadth), S = shortest axis (thickness), C (compact), CP (compact-platy), CB (compact-bladed), CE (compact-elongated), P (platy), B (bladed), E (elongated), VP (very platy), VB (very bladed), VE (very elongated),d. Radius of corners and maximum inscribed circle to calculate particle roundness as suggested by Wadell (1932),e. Photographic and silhouette charts used to evaluate particle roundness, from Powers (1953): A — very angular, B — angular, C — sub angular, D — sub rounded, E — rounded, and, F — well rounded.

researchers quantify roundness of a particle by comparison with standard silhouette charts or photographic images (Figure 1e) Powers (1953).

Surface texture generally refers to the small-scale surface features or the outer physical appearance of a particle (Figure 1a). The existing test procedure ASTM D3398-00 (2000) provides an indirect estimation of intuitive qualities and is described by terms such as rough, smooth, or bumpy surface. It can give useful information on transport mechanism and depositional environment of sediments, although relatively little quantitative work has been done (Evans and Benn, 2004).

3. Image analysis system

Image analysis (digital-sieving) is a process of extracting quantitative information from digital images (Sonka et al., 1999; Gonzalez and Woods, 2007). Over the last few decades research about automatic or

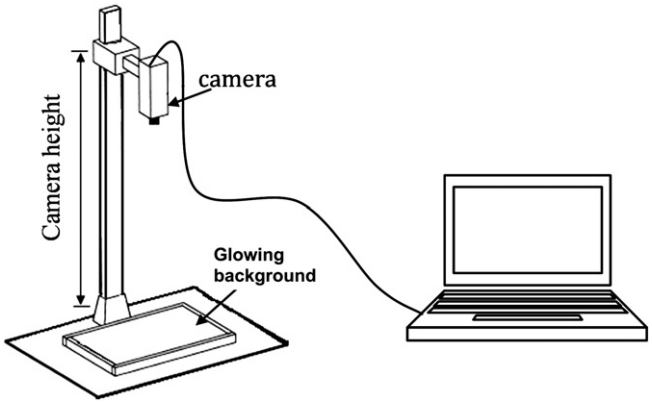

Fig. 2. Schematic diagram of the image acquisition setup; a digital camera connected directly to a computer.

semi-automatic recognition of particles from digital images has developed worldwide (Wang and Bergholm, 1995; Mora et al., 1998; Kwan et al., 1999; Mora and Kwan, 2000; Rao et al., 2001; Taylor, 2002; Maerz, 2004; Fernlund, 2005a, 2005b; Tutumluer et al., 2005; Fernlund et al., 2007; Tafesse et al., 2008, 2009; Tafesse, 2010).

A review of the different means of determining the size and shape of particles using image analysis is made by Wang and Fernlund (1994). In general all image analysis systems entail four basic steps: image acquisition, thresholding, image processing, and data representation.

3.1. Image acquisition

Digital images can be acquired in different ways, most commonly by using scanners and digital cameras. Image quality governs whether or not the images need preprocessing prior to analysis. Advanced preprocessing and image segmentation is often required; whenever the color of the background is similar to the objects or if the particles are touching to each other.

3.2. Thresholding

The first step in image processing is to recognize the object to be analyzed, which is done by identifying the object boundaries from background. This stage of the image processing is called thresholding, where the image is converted to a binary (*bi-level*) image. The thresholding produces a black and white image from the input image, leaving the objects to be measured white and distinguishable from the background. All pixels with gray levels smaller than the threshold value are made equal to "0" (black) while all pixels with gray levels greater than the threshold values are made equal to "255" (white). The choice of the threshold value depends upon the background color and brightness of the particle to be identified in the image.

3.3. Image processing

Image processing is the calculation of the different parameters defined to be measured. Many commercial image processing programs provide pre-defined parameters which can be selected for analyses. However the algorithms used to extract the parameters are not open to the user, which makes the commercial image analysis software less advantageous for researchers who want to know how the parameters are defined. In general, it is important that the parameters are rotationally independent in order to insure reproducible and accurate results. Furthermore the algorithms have to facilitate prompt calculations as well as result in accurate and reproducible measurement of the objects.

3.4. Data representation

Image analysis systems generate an enormous amount of data with respect to the specific parameters chosen. The data output can be automatically transferred to Microsoft Excel or other statistical programs for further evaluation.

4. Existing digital-sieving systems

There are numerous digital-sieving systems used to determine the 3-D size and shape distribution of particles (Fletcher et al., 2003; Maerz, 2004; Fernlund, 2005a, 2005b; Tutumluer et al., 2005). In general the systems can be grouped into two categories; static and dynamic systems. The two systems vary in terms of the instrument setups and algorithms employed to compute the quantitative parameters of a particle.

Kuo et al. (1996) presented static image acquisition method, which uses a transparent Plexiglass rectangular box to hold the particles. The images of the particles are captured in two different ways; either with two cameras positioned in orthogonal directions or by a single camera, in which case the Plexiglass holder is rotated in two perpendicular directions. The particles in the Plexiglass may have different exposure to the lighting condition and the outer end of the particles could create a shadow effect during image acquisition, which would be a problem regarding precision of the measurement of the particle size. The Aggregate Imaging System (AIMS), which was developed by Fletcher et al. (2003), is another static method. In this method particles are placed on a transparent glass tray marked with grid points and their image is acquired in two steps. In the first step a light background is used, which results in a good quality image where the particle appears as a black silhouette with white background. This image is analyzed to determine the major (longest) and intermediate axis of the particle. The second imaging step captures gray level images of the aggregate surface, and is used to compute the minor (shortest) axis of the particle.

Dynamic 3-D image analysis systems often have moving conveyer belt setups. The belt continuously transports the particles towards synchronized cameras placed in orthogonal position. There are two well-known dynamic 3-D-image methods: the University of Illinois Aggregate Image Analyzer (UIAIA) and Wipshape. The UIAIA uses three synchronized cameras to capture the 3-D view of the particles imaged from three orthogonal directions (Tutumluer et al., 2005). The cameras capture the front, top, and side views of the particle. The Wipshape system applies similar principles as of UIAIA. However it uses two synchronized cameras to capture the top and side view image of the particle. Furthermore the particles can be transported to the cameras using either a rotating conveyor belt or a translucent rotating table (Maerz, 2004).

The design and construction of the instruments for 3-D image analysis system are costly and they are not suitable for field application. In most of the existing methods, every particle must be imaged one by one, so that the same particle can be unambiguously identified in the different camera views. The captured images are then processed using software developed specifically for the application to evaluate the predefined parameters.

The different research groups have developed different techniques to measure the 3-D shape and size parameters of the particles; however none of them have been developed for processing particles image both in the laboratory and in the field.

5. New image analysis system: digital photo sieving

A new image acquisition method and image analysis algorithm was developed in order to evaluate the 3-D size and shape of coarse particles (Tafesse et al., 2008; Tafesse, 2010). The placement of the particle was done carefully in two different orientations so that the three main axes (a, b and c) of the particles were imaged. The

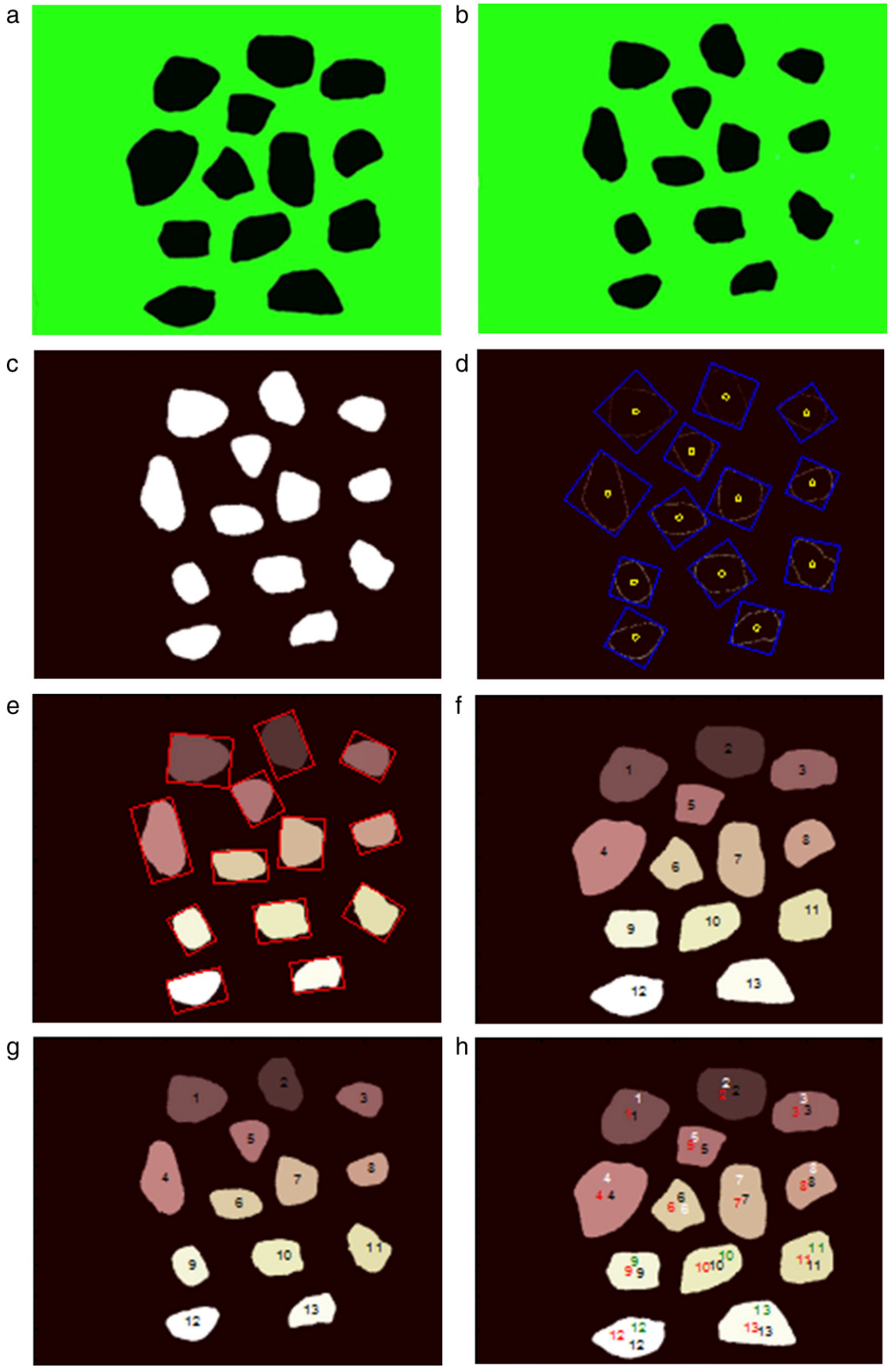
a
b
c
d
e
f
g
h

Table 1
Example of the different parameters measured on12 particles (unit in cm), based on pair of images acquired in two projections.

Particles no.	Lying position							Standing position						
	DLRL	DLRW	LRL (a)	LRW (b_l)	LMBS	Area (A_l)	Area (A_{el})	DSRW	DSRT	SRW (b_s)	SRT (c)	SMBS	Area (A_s)	Area (A_{es})
1	9.67	8.13	9.06	8.12	8.78	57.38	61.73	7.89	4.12	8.05	4.27	7.30	29.08	25.53
2	8.56	6.95	8.71	7.08	8.45	48.97	46.69	7.03	5.80	7.17	5.95	7.17	32.16	32.02
3	10.47	8.74	10.43	8.72	9.92	67.25	71.85	8.59	4.81	8.76	4.87	7.54	32.94	32.43
4	12.45	10.56	12.55	10.63	12.45	108.69	103.29	10.68	7.60	10.91	7.75	10.08	66.29	63.76
5	14.36	10.97	14.10	10.52	13.26	118.75	123.70	11.00	6.85	10.92	6.94	10.29	60.80	59.13
6	13.30	11.58	12.22	11.18	12.16	115.40	121.00	11.23	8.71	11.37	8.71	10.86	80.41	76.85
7	10.79	10.40	9.72	9.11	9.67	71.44	88.08	10.00	4.99	10.12	5.12	7.85	36.93	39.20
8	9.92	8.95	9.84	8.25	9.57	65.71	69.70	9.12	4.98	9.30	5.09	8.01	37.49	35.66
9	9.50	8.03	9.15	8.12	8.84	58.45	59.93	8.51	6.01	8.41	5.76	7.53	37.80	40.17
10	10.20	7.94	9.94	8.06	9.21	58.17	63.63	7.90	4.88	7.97	5.02	7.22	31.87	30.28
11	8.13	7.58	8.10	7.77	7.95	48.21	48.38	7.81	5.64	7.82	5.76	7.05	34.25	34.56
12	11.25	8.28	11.33	8.41	10.84	68.67	73.11	8.27	6.64	8.41	6.79	8.41	44.27	43.14

image analysis program was written in Matlab and the user can access the code in order to optimize parameters which are defined and measured from the particle image.

5.1. Image acquisition

A digital camera connected directly to a computer was used to capture the image of the particles (Figure 2). Thus it was possible to examine the image on the computer screen, in order to ensure high-quality image capturing.

During the image acquisition, a bed of Glow-In-the-Dark beads which hold particles in the required position and create a luminous background was used; thus the technique was named the GID method. Particles were placed in a non-touch situation. A pair of images was taken in two positions in order to determine the 3-D size and shape of the particles. The first image was taken with particles placed in a lying position; where their maximum projected area and the two longest axes (length and width) faced the camera view. The second image was captured after turning the particles orthogonally, which yields the minimum projected area and then enables the calculation of the two smaller axes (width and thickness). Larger particles were placed in the central area of the bed and smaller particles in the peripheries of the camera view, in order to minimize the error which could occur from the shading and tilting effect caused by the angle of the camera view. It is important that the particles are not moved from their relative position between the two images taken in different orientation, to ensure the image analysis proceeds on the same particles (Figure 3a and b).

The bed of glow-in-the-dark beads creates a luminous background which produces a particle silhouette in the image, resulting in high-quality images with good contrast. Between every pair of image captures, the beads are recharged by exposing them to daylight. If the procedure is done indoors a special fluorescence light is required to excite the beads between images.

5.2. Definition of the measured parameters and data presentation

In this study the size and shape of the particles were processed using the new GID program. This image analysis program produced different kinds of output images (Figure 3). It primarily converted the original particle image (Figure 3a, b) into a silhouette by gray level thresholding (Figure 3c). Boundary and geometric centers for each particle were identified and the size of the particle was determined by measuring the dimensions of the circumscribed square and rectangle around the particle in both projections (Figure 3d, e). Finally to obtain 3-D size and shape distribution, the same particles in each of the two images were automatically identified (Figure 3f, g); then the program automatically pair the same particle from the two projection images on the basis of nearest center of geometric coordinates and provide a new identification label (Figure 3h).

5.2.1. Measured parameters

The following parameters were calculated for the pair of pictures taken in the two different positions (Table 1).

5.2.1.1. Lying rectangle length. LRL is the length of longest side of the smallest circumscribing rectangle around the particle's maximum projected area, this dimension considered to be a representative dimension to the longest dimension (a-axis) of the particles.

5.2.1.2. Dominant lying rectangle length. DLRL is length of the longest side of a circumscribing rectangle in the dominant direction around the particle's maximum projected area, which is usually longer than LRL.

5.2.1.3. Lying rectangle width. LRW is the length of shortest side of a circumscribing rectangle around the particle's maximum projected area, the intermediate axis or breadth (b_L) of the particle, is perpendicular to the LRL.

5.2.1.4. Dominant lying rectangle width. DLRW is the length of smallest side of a circumscribing rectangle around the particle's maximum projected area in the dominant direction.

5.2.1.5. Lying minimum bounding square. LMBS is the length of the smallest square that can be circumscribed around the particle's maximum projected area.

5.2.1.6. Standing rectangle width. SRW is the length of longest side of the circumscribed rectangle around the particle's minimum projected area, is termed as intermediate axis or breadth (b_S), in general the value should be very similar to LRW (b_L).

Fig. 3. Input and automatically generated output images by the GID showing the different stages of processing,a. Original particles image (in lying position), the glowing bead background forms a silhouette appearance for the particles,b. Original particles image,(in standing position), light background created by the luminous glow in the dark beads,c. Binary picture (thresholded original image),d. The edge boundary, geometric center and the standing minimum bounding square (SMBS) identified for all particles,e. Minimum bounding rectangle circumscribed around each particle, used to determine the LRL and LRW,f. Identification label marked automatically for every particle in the lying set of picture,g. Identification label marked automatically for every particle in the standing picture set,h. Label identification is marked automatically for every particle in the standing and lying projections. The three identification numbers on the image show the labels identified for the standing and lying position pasted on the lying projection view. Then finally one identification label is generated to calculate the 3-D size and shape parameters.

5.2.1.7. Dominant standing rectangle width. DSRW is the length of longest side of a circumscribing rectangle in the dominant direction around the particle's minimum projected area.

5.2.1.8. Standing rectangle thickness. SRT is the length of shortest side of the circumscribed rectangle around the particle's minimum projected area, this considered to be a representative dimension to the shortest axis (c) of the particle.

5.2.1.9. Dominant standing rectangle thickness. DSRT is the length of smallest side of a circumscribing rectangle around the particle's minimum projected area in the dominant direction.

5.2.1.10. Standing minimum bounding square. SMBS is the length of the smallest square which can be circumscribed around the particle's minimum projected area. This could be visualized as the minimum width of a square sieve opening in the horizontal plane through which the particle can pass through (Fernlund et al., 2007).

Area is measured in two different ways (Table 1). The first (A_l or A_s, l — lying and s — standing positions) is calculated by summing the number of pixel in every connected region of the particle that is bounded by the outer contour (polygon). The other one (A_{el} or A_{es}, l — lying and s — standing positions) is the area of the best fitted ellipse which has the same major axes as the particle in the dominant direction.

The shape parameter for each particle is characterized by the Sneed and Folk three dimensional form indexing method. These values are calculated as a fraction of the three different axial ratios that result in different kinds of form categories. These include ten classes: compact (C); compact platy (CP); compact bladed (CB); compact elongated (CE); platy (P); bladed (B); elongated (E); very platy (VP); very bladed (VB) and very elongated (VE) forms.

5.2.2. Data presentation

The image analysis program automatically generates a summary table, cumulative plots and scatter plots as an output. The axial dimensions, flatness and elongation index of all the particles are presented in a summary table and cumulative curves. On the basis of the index value relationship between the three axes, the form of each particle is plotted on the Sneed and Folk's (1958) triangular diagram.

Fig. 4. Location map of the sampling sites; Bäckseda and Önnestad, in southern part of Sweden.

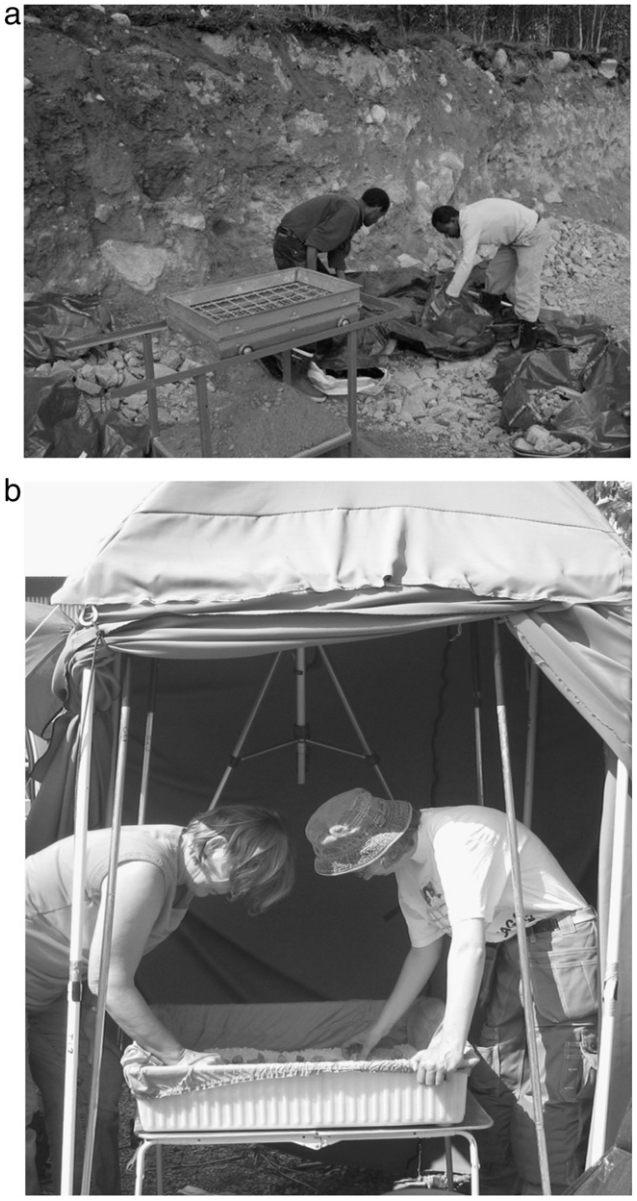

Fig. 5. Photographic illustration of the sample preparation and field image setup,a. Sampling from a road-cut section,b. Image acquisition setup for the field application.

6. Experimental analysis

In order to test the potential applicability of the GID image analysis technique, four samples were studied. The samples were obtained from glacial till at two locations in the southern part of Sweden (Figure 4). They were of two types: three samples composed of coarse gravel (2 to 6 cm size) obtained from the Önnestad site and one sample composed of cobbles (6 to 20 cm size) obtained from the Bäckseda site (Figure 5a).

A total of 1250 clasts were imaged and sieved in this study; 84 clasts from the cobble sized sample and an average of 400 clasts from each of the three coarse gravel samples. The images of the samples were captured in the field inside of a portable darkroom (Figure 5b). The darkroom was made of inexpensive, lightweight and light-impenetrable cloth; supported by lightweight plastic poles. It was accessible from all sides, for placing the particles on the bed of glow-in-the-dark beads. The height of the camera was about 1.5 m, and the photograph covered a base area of 1 m by 0.80 m. The number of particles in one image varied between 15 larger particles (size on the order of 6 to 20 cm) and 150 smaller particles (size on the order of 2 to 6 cm). After imaging was completed, the samples were sieved. The cobble sample was sieved using square templates of size 90.5, 128, and 181 mm; whereas the three coarse gravel samples were mechanically sieved using half phi sieves, 25, 31.5 and 45 mm size.

7. Results

The grain size distributions of the clasts in the different samples are shown by cumulative curves in log-normal plots (Figure 6). The image analysis results for size distribution of the sample used cumulative volume, rather than cumulative mass which is used in sieve analysis. There are various methods used to determine volume of particles from measurements obtained from image analysis (Mora et al., 1998; Mora and Kwan, 2000; Rao et al., 2001; Maerz, 2004; Tutumluer et al., 2005). In this study the volume was obtained by using a simple formula; the product of the maximum projected area by thickness, where the thickness is the standing rectangle width (SRW). The cumulative distributions of the standing minimum bounding square (SMBS, see previous definition) of the four samples (Figure 6a–d) show similarity to the sieve analysis curve. In contrast the cumulative distributions of intermediate axes (b_L) do not agree with the sieve analysis curve.

The calculated volume, obtained by the product of area by thickness, normally would yield a much larger value than the actual volume. The actual volume of the sample was back calculated by using a correction factor (λ), as described in the formula by Mora et al. (1998).

$$\lambda = M/\rho \sum_{i=1}^{n} (area * thickness) \tag{2}$$

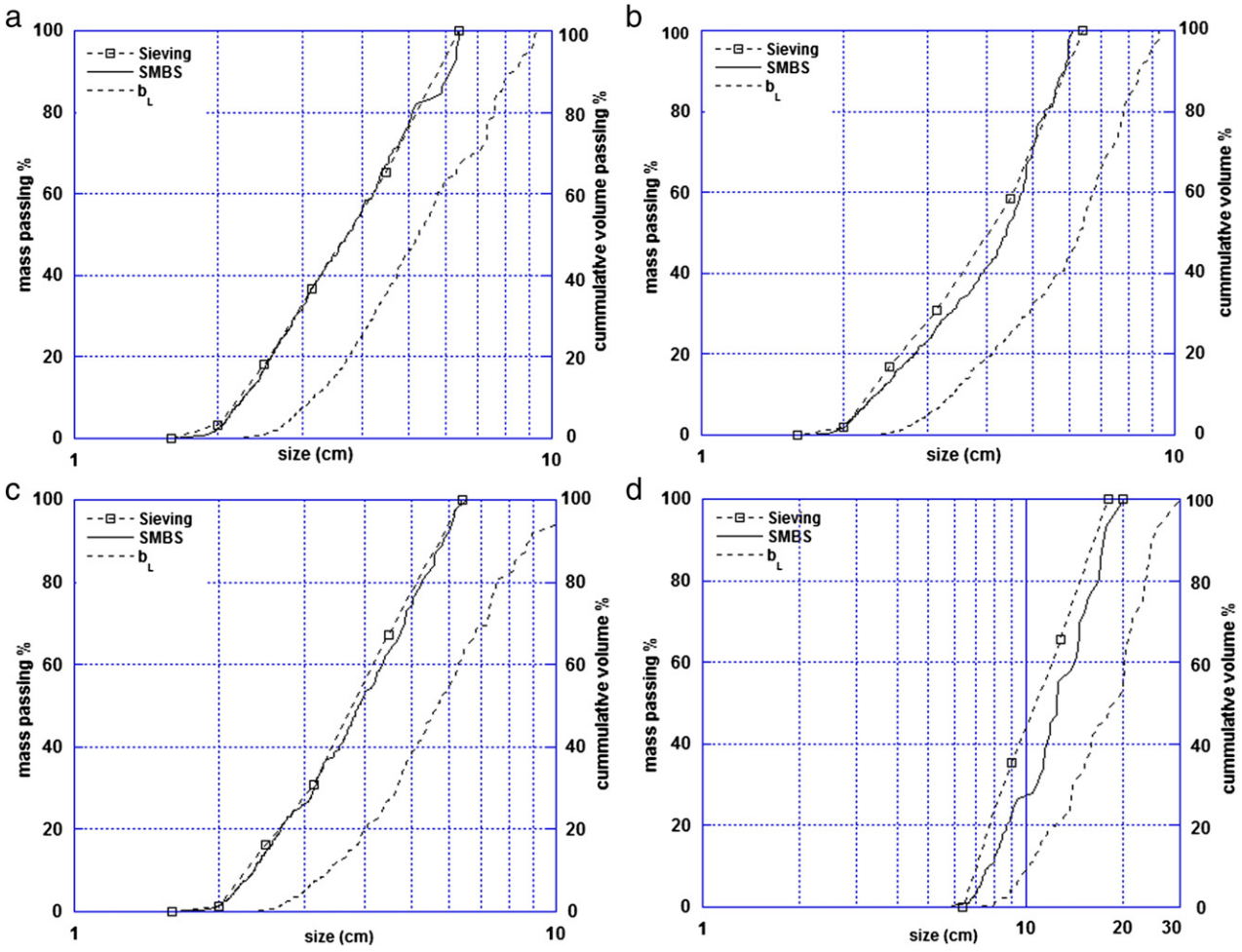

Fig. 6. Relationship of particle size distribution based on sieve analysis and image analysis (the minimum bounding square (SMBS) and intermediate axis (b_L) plotted in cumulative diagram).a. Önnestad sample 1,b. Önnestad sample 2,c. Önnestad sample 3,d. Bäckseda sample.

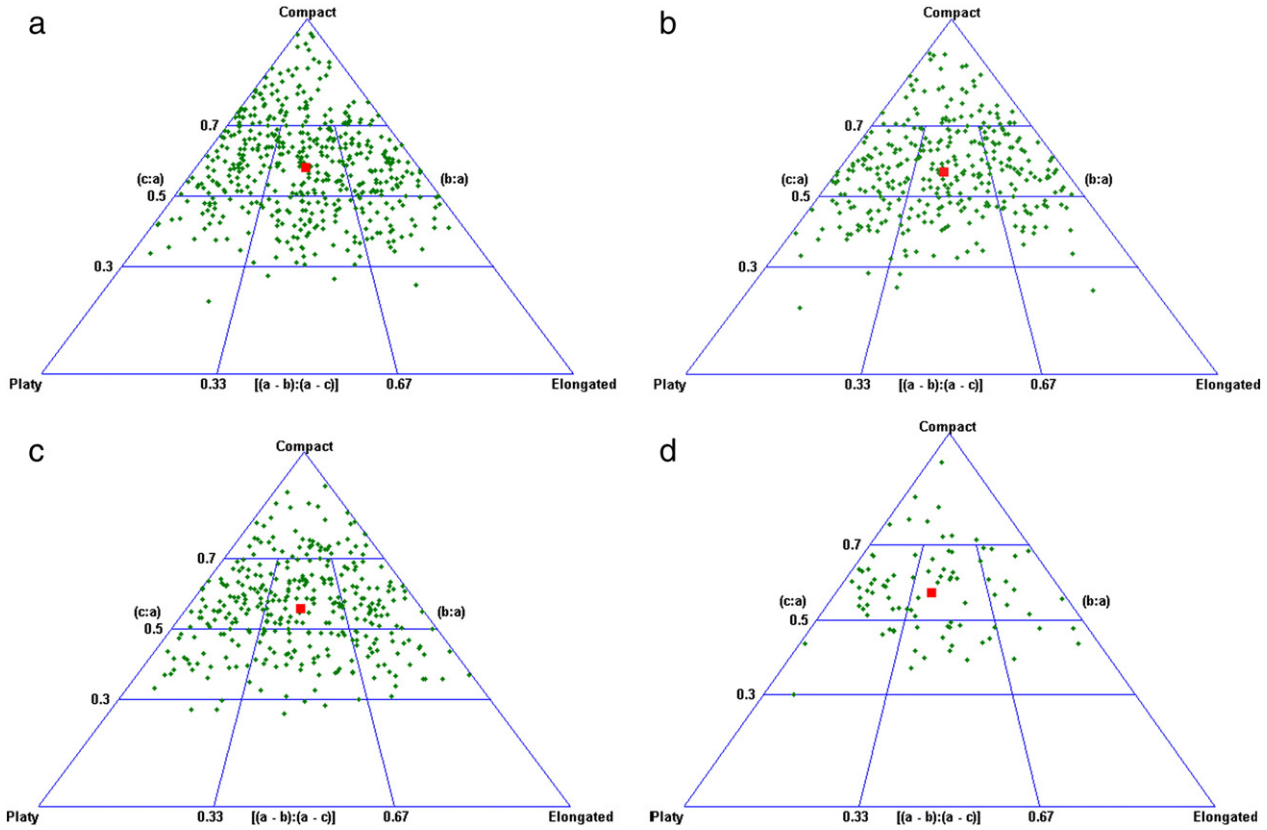

Fig. 7. 3-D form index distribution for the four samples, plotted in the Sneed and Folk triangular diagram, the square shaped marker (in red color) represent the average value for the sample. a. Önnestad sample 1,b. Önnestad sample 2,c. Önnestad sample 3,d. Bäckseda sample.

Since the total mass (M) of our sample was known and by assuming an average density (ρ) as 2.8 g/cm^3; we calculated the correction factor (λ) for our samples; the average value was 0.32.

However the position of the SMBS curves in the distribution plot which was obtained based on both cumulative volumes was identical. This is because the cumulative volume in the y-axis was normalized; therefore the correction factor used for evaluating the corrected volume will be canceled out, during the calculation of the cumulative percent distribution (Fernlund et al., 2007).

The distribution of the 3-D form index for the four samples was plotted in the Sneed and Folk triangular plot (Figure 7), and the percent distribution was summarized (Table 2). The clasts from the Bäckseda sample were predominately compact-platy (CP) (30%) and there were no extreme shapes (VB, VE, and VP). The shapes of the clasts from the three Önnestad samples were similar to one another. There was no single shape class which was most predominate but the B, C, CB, CE and CP were nearly equally represented and the samples contained a few particles with extreme shapes (VB, VE, VP). Thus there is a clear difference in shape distribution between the Önnestad and Bäckseda sites.

Table 2
Shape distribution summary in percent.

Form types	Önnestad sample 1	Önnestad sample 2	Önnestad sample 3	Bäckseda sample
Bladed (B)	13.15	11.94	13.37	17.24
Compact (C)	19.21	14.93	13.37	10.34
Compact bladed (CB)	18.79	19.10	20.93	17.24
Compact elongated (CE)	16.28	17.01	14.24	13.79
Compact platy (CP)	17.33	18.81	18.02	29.89
Elongated (E)	7.93	6.87	9.88	4.60
Platy (P)	6.47	9.85	8.43	6.90
Very bladed (VB)	0.42	0.60	0.87	0.00
Very elongated (VE)	0.21	0.30	0.00	0.00
Very platy (VP)	0.21	0.60	0.87	0.00

8. Discussion and conclusions

This study presents a novel method, which is simple and inexpensive to use, for field imaging of particles. The suitability of the image acquisition method for application in the field could make it attractive for analyzing large sample sizes which are statistically representative for coarse-grained gravel and pebble sized clasts. The time required for the image acquisition and processing in our method was relatively small, which depends on the number of particles imaged at one time. It takes a few seconds per particle to place in the two projections, about 15 min to capture the two set of images (in both lying and standing positions) of about 150 particles. A statistically representative bulk sample size for the study of coarse gravel and cobble, size up to 20 cm, is one metric tonne (Church et al., 1987; Påsse, 2003). In this study each sample of till consisted of one metric tonne. All the particles >2 cm and <20 cm were studied; more than 1200 coarse gravel and cobble particles. It is very expensive to transport such large samples to the laboratory and thus a field method is an economical alternative. The GID method yields detailed information about the 3-D size and shape of every particle in the sample. Such detailed information can be very useful for interpreting sediment genesis.

The GID image acquisition method provides good quality images of the particles (Figure 5a, b), with good contrast between the background and the particles. This enables easy thresholding without the need for preprocessing which means that the accuracy of the results is not influenced during image segmentation and that the time required for the analysis is shorter than if preprocessing is needed. The image analysis software is developed in Matlab which allows the user to have control over the measured parameters and can easily be implemented by other

researchers. Whereas commercial image analysis programs do not enable the user to understand what is being measured and how the parameters are being computed.

In contrast, other image acquisition methods, such as the University of Illinois aggregate image analyzer (UIAIA) and the Wipshape imaging system, require sophisticated and expensive equipment (Maerz, 2004; Tutumluer et al., 2005). The samples must also be transported to the laboratory which increases the cost. The equipment used in these two methods implements imaging of just one particle at a time which means that the analysis is done for each particle individually. This takes more time than the GID method where several particles are included in one image and the analysis is done simultaneously for all the particles.

Many of the existing image analysis programs determine the particle size distribution using the three particle axes (a, b and c axis). It is common to use different conversion factors to correct the b-axis and "make it fit" with the sieve analysis curves of the granular materials (Mora et al., 1998). However it does not fit for the entire curve but usually fit the first to third quartiles and the tails usually do not fit well. This factor varies for the different aggregate materials from different sources and must be derived for each material type. Therefore there would not be a single factor that could be used for sediment such as glacial till clasts which consist of different rock fragments from different sources. It is thus important to be able to measure directly a parameter that yields sieve size without needing a correction factor. Fernlund et al. (2007) defined the standing minimum bounding square (SMBS) and suggest it was equivalent to sieve size. The results of this study support this conclusion as the SMBS distributions are similar to the sieving curves (Figure 6). No correction factor is needed but this is a direct measure. This would make the GID attractive for construction Engineers, who produce aggregate mix batches for asphalt and concrete based on mechanical sieve-size distribution and not from the axial dimensions of the particles.

In order to address the potential problem associated with small variations in the focal length a related research work has been done in (Lindström, 2010; Tafesse et al., submitted for publication). The research was done on 25 particles with size from 2 to 20 cm. Images were taken from 10 different heights: i.e. 100, 110, 120, 130, 160, 170, 180, 190 and 200 cm. At each camera height 10 images were taken. The particles were put in different places for each of the 10 images. This means that a total of 100 pictures were used in the analysis. The study showed minor variation in the size and shape distribution, between the 100 images. This variation could be attributed to the apparent shape change which could occur when the camera views the particle in different angle, when they are placed at different positions.

Although image analysis yields an exact value for the parameters there are still several sources of error or uncertainty in the results. The orientation of the particle imaged will result in size and shape variations. The quality of the images will also influence the results. If the images are not good quality then the results will be affected. In these respects image analysis results are not absolutely accurate. However, when compared with the indirect method of sieving, where the size is only indirectly measured image analysis yields more information about each particle.

Acknowledgment

The funding was provided by the Swedish Research Council for Environment, Agricultural Sciences and Spatial Planning (Formas) is gratefully acknowledged. We would also like to acknowledge for the comments obtained from the anonymous reviewers; and wish to express our gratitude to Mimmi and Katrin for proof reading and commenting the paper.

References

Allen, T., 1968. Particle Size Measurement. Chapman and Hall, London.
Al-Rousan, T., Masad, T., Tutumluer, E., Pan, T., 2007. Evaluation of image analysis techniques for quantifying aggregate shape characteristics. Construction and Building Materials 21, 978–990.
ASTM designation D3398-00, 2000. American Society for Testing and Materials, Standard test method for index of aggregate particle shape and texture. 04.03, West Conshohocken, PA.
Blum, H., 1967. A transformation for extracting new descriptors of shape. In: Wathen-Dunn, W. (Ed.), Models for the Perception of Speech and Visual Form. MIT Press, Cambridge, Massachusetts, pp. 362–380.
Brewer, R., 1964. Fabric and Mineral Analysis of Soils. Wiley, Chichester.
Bunte, K., Abt, S.R., 2001. Sampling surface and subsurface particle-size distributions in wadable gravel and cobble-bed streams for analyses in sediment transport, hydraulics, and streambed monitoring. United States Department of Agriculture, General Technical Report 74.
Church, M.A., McLean, D.G., Wolcott, J.F., 1987. River bed gravels: sampling and analysis. In: Thorne, C.R., Bathurst, J.C., Hey, R.D. (Eds.), Sediment Transport in Gravel-Bed Rivers. Wiley, Chichester, pp. 42–88.
Drik, G., 2008. Technique to measure grain size distribution of loamy sediment: a comparative study of ten instruments for wet analysis. Sedimentology 55, 65–96.
Evans, D.J.A., Benn, D.I. (Eds.), 2004. A Practical Guide to the Study of Glacial Sediments. Oxford University Press, London.
Fernlund, J.M.R., 1998. The effect of particle form on sieve analysis: a test by image analysis. Engineering Geology 50, 111–124.
Fernlund, J.M.R., 2005a. Image analysis method for determining 3-D size distribution of coarse aggregates. Bulletin of Engineering Geology and the Environment 64, 159–166.
Fernlund, J.M.R., 2005b. Image analysis method for determining 3-D shape of coarse aggregate. Cement and Concrete Research 35, 1629–1637.
Fernlund, J.M.R., Zimmerman, R.W., Kragic, D., 2007. Influence of volume/mass on grain-size curves and conversion of image — analysis size to sieve size. Engineering Geology 90, 124–137.
Fletcher, T., Chandan, C., Masad, E., Sivakumar, K., 2003. Aggregate Imaging System (AIMS) for characterizing the shape of fine and coarse aggregates. Transportation Research Record 1832, 67–77.
Folk, R.L., 1966. A review of grain size parameters. Sedimentology 43, 910–1010.
Fripp, J.B., Diplas, P., 1993. Surface sampling in gravel streams. Journal of Hydraulic Engineering 119, 473–490.
Gomez, B., Dowdeswell, J.A., Sharp, M., 1988. Microstructural control of quartz sand grains shape and texture: implications for the discrimination of debris transport pathways through glaciers. Sedimentary Geology 57, 119–129.
Gonzalez, R.C., Woods, R.E., 2007. Digital Image Processing, third ed. Prentice Hall.
Gordon, N.D., McMahon, T.A., Finlayson, B.L., 1992. Stream hydrology. An introduction for Ecologists. John Wiley and Sons, Chichester, GB. 526 pp.
Griffith, J.C., 1967. Scientific Method in Analysis of Sediments. McGraw-Hill, New York.
Hayakawaa, Y., Oguchib, T., 2005. Evaluation of gravel sphericity and roundness based on surface-area measurement with a laser scanner. Computers and Geosciences 31, 735–741.
Ibbeken, H., Denzer, P., 1998. Clast measurement; a simple manual device and its semi-automatic electronic equivalent. Journal of Sedimentary Petrology 58, 751–752.
Krumbein, W.C., 1941. Measurement and geological significance of shape and roundness of sedimentary particles. Journal of Sedimentary Petrology 11, 64–72.
Krumbein, W.C., Pettijohn, F.J., 1938. Manual of Sedimentary Petrography. D. Appleton-Century Company, Inc., New York.
Kuo, C.Y., Frost, J.D., Lai, J.S., Wang, L.B., 1996. Three-dimensional image analysis of aggregate particles from orthogonal projections. Transportation Research Record 1526, 98–103.
Kwan, A.K.H., Mora, C.F., Chan, H.C., 1999. Particle shape analysis of coarse aggregate using digital image processing. Cement and Concrete Research 29, 1403–1410.
Lindqvist, J.E., Åkesson, U., 2001. Image analysis applied to Engineering Geology, a literature review. Bulletin of Engineering Geology and the Environment 60, 117–122.
Lindström, H., 2010. Rock Properties measurement using image processing. TRITA-LWR Master's thesis, 10:28.
Maerz, N.H., 2004. Technical and computational aspects of the measurement of aggregate shape by digital image analysis. Journal of Computing in Civil Engineering 18, 10–19.
Masad, E., Button, J., Papagiannakis, T., 2000. Fine aggregate angularity: automated image analysis approach. Transportation Research Record 1721, 66–72.
Masad, E., Olcott, D., White, T., Tashman, L., 2001. Correlation of fine aggregate imaging shape indices with asphalt mixture performance. Transportation Research Record 1757, 148–156.
Masad, E., Al-Rousan, T., Button, J., Little, D., Tutumluer, E., 2007. Test methods for characterizing aggregate shape, texture, and angularity. National Cooperative Highway Research Program (NCHRP) Report 555. Transportation Research Board, Washington, D.C.
Mora, C.F., Kwan, A.K.H., 2000. Sphericity, shape factor, and convexity measurement of coarse aggregate for concrete using digital image processing. Cement and Concrete Research 30, 351–358.
Mora, C.F., Kwan, A.K.H., Chan, H.C., 1998. Particle size distribution analysis of coarse aggregate using digital image processing. Cement and Concrete Research 28, 921–932.
Påsse, T., 2003. Methods for estimating total grain size distribution in till. Swedish Geological Survey (SGU) research seminar documentation, pp. 9–10.
Pettijohn, F.J. (Ed.), 1984. Sedimentary Rocks. S.K. Jain, India.
Powers, M.C., 1953. A new roundness scale for sedimentary particles. Journal of Sedimentary Petrology 23, 117–119.
Rao, C., Tutumluer, E., 2000. A new image analysis approach for determination of volume of aggregates. Transportation Research Record 1721, 73–80.
Rao, C., Tutumluer, E., Stefanski, J.A., 2001. Coarse aggregate shape and size properties using a new image analyzer. ASTM Journal of Testing and Evaluation 29, 79–89.
Rao, C., Tutumluer, E., Kim, I.T., 2002. Quantification of coarse aggregate angularity based on image analysis. Journal of the Transportation Research Board 1787, 117–124.

Rice, S.P., Church, M., 1996. Sampling fluvial gravels: bootstrapping and the precision of size distribution percentile estimates. Journal of Sedimentary Research 66, 654–665.
Sneed, E.D., Folk, R.L., 1958. Pebbles in the lower Colorado River, Texas, a study in particle morphogenesis. Journal of Geology 66, 114–150.
Sonka, M., Hlavac, V., Boyel, R. (Eds.), 1999. Image Processing, Analysis and Machine Vision, Second ed. Pacific Grove, California.
Syvitski, J.P.M. (Ed.), 1991. Principle, Methods and Application of Particle Size Analysis. Cambridge University Press, London.
Tafesse, S., 2010. Physical properties of coarse particles in till coupled to bedrock composition based on new 3D image analysis method, TRITA-LWR.LIC 2047, Licentiate thesis.
Tafesse, S., Fernlund, J.M.R., Bergholm, F., Arvidsson, M., 2008. New method for 3-D size measurements of particles using image analysis. The 33rd International Geological Congress, Oslo, Norway.
Tafesse, S., Fernlund, J.M.R., Bergholm, F., Arvidsson, M., 2009. New methods to analyze glacial till clasts roundness and texture. The 27th IAS Meeting in Alghero, Italy.
Tafesse, S., Fernlund, J.M.R, Bergholm, F, Sun W., submitted for publication. Evaluation of image analysis methods used to quantify particle angularity. Sedimentology.
Taylor, M.A., 2002. Quantitative measures for shape and size of particles. Powder Technology 124, 94–100.
Tutumluer, E., Pan, T., Carpenter, S.H., 2005. Investigation of Aggregate Shape Effects on Hot Mix Performance Using an Image Analysis Approach. Civil Engineering Studies, Transportation Engineering University, Illinois, Urbana-Champaign.
Wadell, H., 1932. Volume, shape, and roundness of rock particles. Journal of Geology 40, 443–451.
Wadell, H., 1935. Volume, shape and roundness of quartz particles. Journal of Geology 43, 250–280.
Wang, W., Bergholm, F., 1995. Moment based edge density for automatic size inspection. Proceedings of the 9th Scandinavian Conference on Image Analysis, Uppsala, Sweden.
Wang, W.X., Fernlund, J.M.R., 1994. Shape Analysis of Aggregates: Application with Image Analysis System. Report No. 2 Department of Civil and Environmental Engineering, KTH, Stockholm.
Wang, L.D., Park, J., Mohammad, L., 2005. Quantification of morphology characteristics of aggregate from profile images. Journal of Materials Science in Civil Engineering 17, 498–504.
Zingg, T.H., 1935. Beitrage zur schotteranalyse: Schweizerische Mineralogische und Petrographische Mitteilungen. Swiss Bulletin of Mineralogy and Petrology 15, 38–139.